

Postprint of: Andrzejczyk R., Kowalczyk T., Kozak P., Muszyński T., Experimental and theoretical study of a vertical tube in shell storage unit with biodegradable PCM for low temperature thermal energy storage applications, APPLIED THERMAL ENGINEERING, Vol. 183, Part 1 (2021), 116216, DOI: [10.1016/j.applthermaleng.2020.116216](https://doi.org/10.1016/j.applthermaleng.2020.116216)

© 2020. This manuscript version is made available under the CC-BY-NC-ND 4.0 license <http://creativecommons.org/licenses/by-nc-nd/4.0/>

Experimental and theoretical study of a vertical tube in shell storage unit with biodegradable PCM for low temperature thermal energy storage applications

Rafal Andrzejczyk¹, Tomasz Kowalczyk², Przemysław Kozak¹, Tomasz Muszyński¹

¹Gdansk University of Technology
Narutowicza 11/12, 80-233 –Poland
Phone: 58 347 18-03

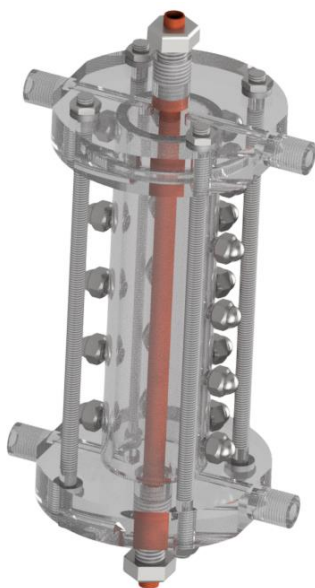
²Fluid Machinery Institute
Gdansk Narutowicza –Poland

email: rafal.andrzejczyk@pg.edu.pl

Highlights

- Modular experimental thermal energy storage heat exchanger and test section design
- Validation of coconut oil thermophysical properties
- Time dependent temperature and heat transfer characteristics
- Simplified TES response model

Graphical abstract



Keywords: melting, solidification, phase change material (PCM), coconut oil

Abstract

This article presents the experimental investigations of coconut oil based TES module for HVAC applications in the ambient and-sub ambient temperature range. To properly study this problem modular experimental module and test loop were developed. The special attention has been paid at study the physical mechanism of melting/solidification process for natural substance (coconut oil) with is seems to be perspective for used in thermal energy storage systems. It has been highlight that melting/solidification process is much more complex for non-eutectic mixtures and there are limited analytical models witch could be used to design TES working with such substances. Due to the limit of literature data for thermophysical properties of coconut oil own experimental data has been conducted.

Article presents both visual and thermal characteristics of melting and solidification process. It has been conformed the strong influence of natural convection phenomena at the melting process. What is more it has been observed that in case of coconut oil it is better to talk about appearance melting temperature than melting temperature. The experimental analysis confirmed that appearance melting temperature is a function of radial distance from heat source. In case of solidification the influences of natural convection is reduce quickly due to increasing domination of conduction heat transfer mechanism. For the solidification temperature profiles are characteristic the occurrence of sub cooling temperature. The level of temperature drop in sub cooling is a function of radial distance from heat source. It has been also confirmed that in case of melting as well as solidification process the shape of phase-change profile seems to forms an truncated cone (in case of melting inverted).

In order to validate engineering approach to vast discrepancies in the literature data own experiment has been evaluated with simple mathematical model to verify the applicability of the literature data in system behavior prediction. Based on the best fit approach the parameters thermal resistance of the module $R = 1.3\text{W/K}$ was found. Additionally the latent heat of the coconut oil of 178 kJ/kg with Gaussian distribution ($\sigma = 1.1$) for melting in temperature of 25°C and solidification in 21°C . The proposed correlation can be easy used to optimize latent thermal energy storage cooperated with HVAC system.

Nomenclature

a – diffusivity, m^2/s

C – specific heat, J/kgK

C_v - volumetric specific heat capacity, J/m^3

F^* – Gauss function

G – gravity acceleration, m^2/s



h_{ls} – latent heat, kJ/kg

\dot{m}_c – mass flux of cooling water, kg/s

M – mass, kg

T – temperature, °C

R – radius, m

R_{th} – thermal resistance, W/K

Q – amount of heat, J

\dot{Q} – heat flux, W,

Acronyms

CCD – fast picture camera with charge-coupled device

HVAC – heat ventilation air conditioning system

PMMA – poly(methyl methacrylate)

PCM – phase change materials

TES – thermal energy storage

Greek symbols

λ – thermal conductivity, W/mK

μ – dynamic viscosity, Pas

σ – Gaussian distribution,

τ – time, s

Subscripts

m – melting,

ls – phase change

r – end cooling,

s – subcooling,

w – wall

0 – initial

1. Introduction

Currently one of the biggest branches of the international economy are heating, ventilation and air conditioning systems. Due to the increasing concerns of the community, many global companies focused on reducing the environmental impact of their products. That impact is in one hand involved with kind of working fluids inside the installations, on the other hand with the demand for minimizing primary energy consumption. It is clear that there is a strong need for environmentally friendly solutions for energy saving. One of the possibilities of energy saving is to minimize peak energy consumption by the installation [1], it is so-called peak



shifting. The thermal energy storage (TES) system can shift the demand for cooling/heating in time. According the literature for air-cooled refrigeration systems if the condenser temperature raised by 1K the COP of such system drops by around 3% [2]. So it is obviously that reducing the condenser temperature is high demand for example by cooperation of HVAC system with thermal energy storage system [3]. It is well known from open literature there are three main kinds of thermal energy storage systems: sensible, latent and thermochemical. One of the most popular kinds is the latent heat storage system due to the high density of energy and nearly constant temperature of discharging/charging of thermal storage [4,5]. There are many studies in open literature concerning different kinds of phase change materials (PCMs) as acid facts, esters, alcohols, paraffin [6].

However, the cheapest and easiest to available commercially are raw materials like animals and organic fats e.g. coconut oil. Coconut oil is available in the marketplace as virgin coconut oil and refined coconut oil. Both of these oil kinds have a good shelf life (2 years for virgin oil and 5 years for refined one) [7]. What is more important these substances are non-toxic can be sustainable, and abundant in nature. It should be stressed that coconut palm can absorb and use saltwater during growth [8]. It is a big advantage of that plant due to limited resources of sweet water in the world.

Generally most of the PCM materials characterized by a low value of thermal conductivity. Due to that fact it is crucial to optimize the geometrical form of a thermal magazine. Several experimental studies have been focused on used fins to enhance the efficiency of charging/discharging latent energy storage systems. Choi and Kim [9] concluded that circular fins increase the uniformity of the radial temperature gradient compared to the unfinned tube. What is more, the ratio of heat transfer coefficient between finned and the unfinned tube is about 3.5 Pizollato et al. [10] used a topology optimization and multi-phase computation and fluid dynamics to optimization fins shape for latent heat thermal energy storage units. Authors have shown in their study that for optimal fins geometry it is possible to reduced charging time at about 27% for 95 % of the total storage capacity of PCM. The results have been worse for solidification (discharging of the storage) the reduction of time was close to 11%. The authors highlighted that it is very important to include fluid flow in the calculation methodology to properly optimize the shape of the latent thermal energy storage unit. They concluded that the optimal geometry for melting is different from geometry optimized for solidification. However, it is worth noting that the proposed geometrical shape of the heat exchanger is hard to produce from a technical point of view. The easiest and still popular construction of thermal energy storage units is an annular storage magazine. The symmetrical



system simple to analyze and manufacturing. What is more in many studies, to simplify calculations, are used this construction as a model to optimization shell and fined tubes heat exchanger [11,12]. Many studies presented evidence for clear influences of fluid movement, natural convection, for melting/solidification phenomena [13]. Mao et al. [14] proposed a new truncated cone shell and tube thermal energy storage system to enhance heat transfer by taking to account natural convection. Authors have shown in their study that new truncated cone construction of magazines would significantly reduce charging time above 32% and discharging time above 21%.

In study by Hosseini et al. [15] the effect of longitudinal fins in a double pipe heat exchanger containing PCM is observed during charging process. Experiments were performed with eight rectangular fins mounted around the horizontal heat carrying tube. Results showed that fins extension leads to the shorter melting time.

Zhao and Tan [16] proposed integrated phase change material in shell-and-tube based thermal storage system with conventional air-conditioner to increase cooling coefficient of performance. The thermal storage unit in the study used water for charging and air for discharging loop. Authors evaluated the effects of varying heat transfer fluid inlet temperature, mass flow rate and fin geometry on the thermal storage performance. The results showed decreased condenser temperature resulting in increased coefficient of performance up to 25% compared to the nominal parameters. Xiaohu Yanga et al. [17] proposed a novel TES with PCM filled by metal foams with gradient in pore parameters as a possible thermal enhancement techniques. They presented physical and numerical studies to predict melting front evolution as well as temperature and velocity fields. It has been confirmed numerically by the authors that the positive gradient in porosity can provide better increase heat transfer in PCM volume than uniform and negative gradient cases. The reduction of melting time was higher than 17%. What is more authors recommended optimization on gradient in porosity of 0.89-0.95-0.98 to further reduce the full melting time by 21,1%. In the next article Xiaohu Yanga et al. [18] experimentally investigated a novel fin-foam structure to enhanced solidification latent thermal energy storage. A numerous of geometrical parameters of proposed structure have been experimentally studied. As a results it has been confirmed that fin-foam structure make improvement of heat transfer intensification during solidification of water by 28,35%. It was also stress that insulation adhesive influences could be neglected in case of the accuracy at pore scale temperature measurements.

In the open literature it can be found also an experimental and numerical study concerning a hybrid techniques for performance increase such of latent heat thermal energy stories using



two or more techniques. Mahdi et al.[19] have been revised numerous experimental and numerical studies focused of hybrid enhancement techniques for application in latent thermal energy storages. The authors highlight that the optimal increase of the energy storage performance is achieved by the application of hybrid techniques like the heat pipe with fins or metal foam. It has been also noted that use of nanoparticles with other enhancement technique (e.g. fins or metal foam) is better than use only nanoparticle. In their next study Mahdi et al.[20] presented their the novel fin configuration as perspective enhancement technique for triplex-tube heat exchanger with phase change materials working through simultaneous heat storage and recovery. In the study the fin geometries have been optimized by numerical investigations. What is more the enhancement of heat performance of heat exchanger by adding nanoparticles to PCM has been also analyzed. The numerical results confirmed that the optimizes fin geometries is better than incorporating nanoparticles to the volume filled by PCM.

The another way to enhancement energy storage systems performance is to use multiple PCMs with different melting temperature. In real working condition the temperature differences between PCM and working fluid decrease if there is only one material used with absorbed the heat. To diminish decrease of heat transfer one way is to use a multi PCM. Zhipei Hu et al. [21] numerical investigation possible to enhance heat transfer in latent energy storage unit. Authors compare of thermal performance traditional shell-and-tube module with novel geometry of frustum-shaped filled by multiple PCM. They have been discovered that novel geometry filled by multiple PCM reduced storage time by 21,5% to 47,5% respectively. H.A. Adine and H. El Qarnia [22] have been numerically studied shell and tube thermal energy storage unit filled by two kinds of PCM. The article presents a mathematical model to predict behavior and performance of module filling by two kinds of PCM and single PCM respectively. The results indicated that only for grater water inlet temperature the module wit multi PCMs is more effective.

Marcello De Falco et al. [23] have experimentally investigated possible to use PCM storage unit to increase efficiency of chiller cooperated with civil air conditioning system. The article presents results for a 5 kWh prototype. Also the mathematical model has been obtained and validated with experimental results. What is more that proposed theoretical correlation has been used to optimize working parameters of the TES unit. It has been noted that such optimization can lead to obtained a minimum loading time for TES equal to 54 minute. It has been confirmed by simulations the possibility to cooperated of proposed latent thermal energy magazine with system characterized by high charging/discharging power and



possibility e.g. HVAC installations in office or residential buildings. Wen-Shing Lee et al.[24] proposed in their study using the partial swarm algorithm to optimization of ice-storage air-conditioning system. The study presented also strategies for system operating by the use of minimal life cycle cost as the objective function. Authors indicated that their model can be easy to adopted to optimize parameters of HVAC system cooperated with TES system.

Despite the fact that many experimental and numerical studies have been done on melting/solidification, not many of them were focused on natural convection influence.

What is more most of the studies in the open literature have been concerned on eutectic mixtures or single compound substances. This study presented physical analysis of melting/solidification process for non-eutectic mixtures and the simple analytical models witch could be used to design TES working with such substances. Thermal energy storage for hot water or heating systems using low temperatures has been thoroughly developed. However, until this present paper, limited attention has been paid to TES for HVAC applications in the ambient and-sub ambient temperature range.

Still currently the main technological problems to use TES in energetic systems is low heat transfer intensity in PCM volume [23]. To properly study this problem modular experimental module in typical shell-and tube geometry and test loop were developed. By presented in the study experimental module geometry it is easy to observed the dynamics of charging/discharging processes and to explore physical nature of the problem with slow phase transition during melting/solidification processes. What is more most of the engineering systems employ cylindrical pipes and the heat losses from such geometries are low. According the literature the latent thermal energy storage systems in form of shell and tube unit has been most intensely analyzed [25].

The experimental work presented leads to obtaining heat transfer to PCM volume for the condition of constant wall temperature. The constant wall parameter has been chosen to model the directly cooperation between TES and condenser/evaporator in refrigeration system. That parameter is also very common to use in many analytical and numerical modules developed to simulations melting/solidification process. It is allow to simplification of physical modeling and to directly compare experimental results with calculation results carried out by proposed analytical model.

It has been conducted experimental investigations of selected thermophysical parameters of PCM to validate literature data.



2. Experimental setup

2.1 Description of experimental loop

Figure 1 shows a scheme of the test section of the heat storage tank, enabling determination of the amount of heat supplied / received from the phase change material.

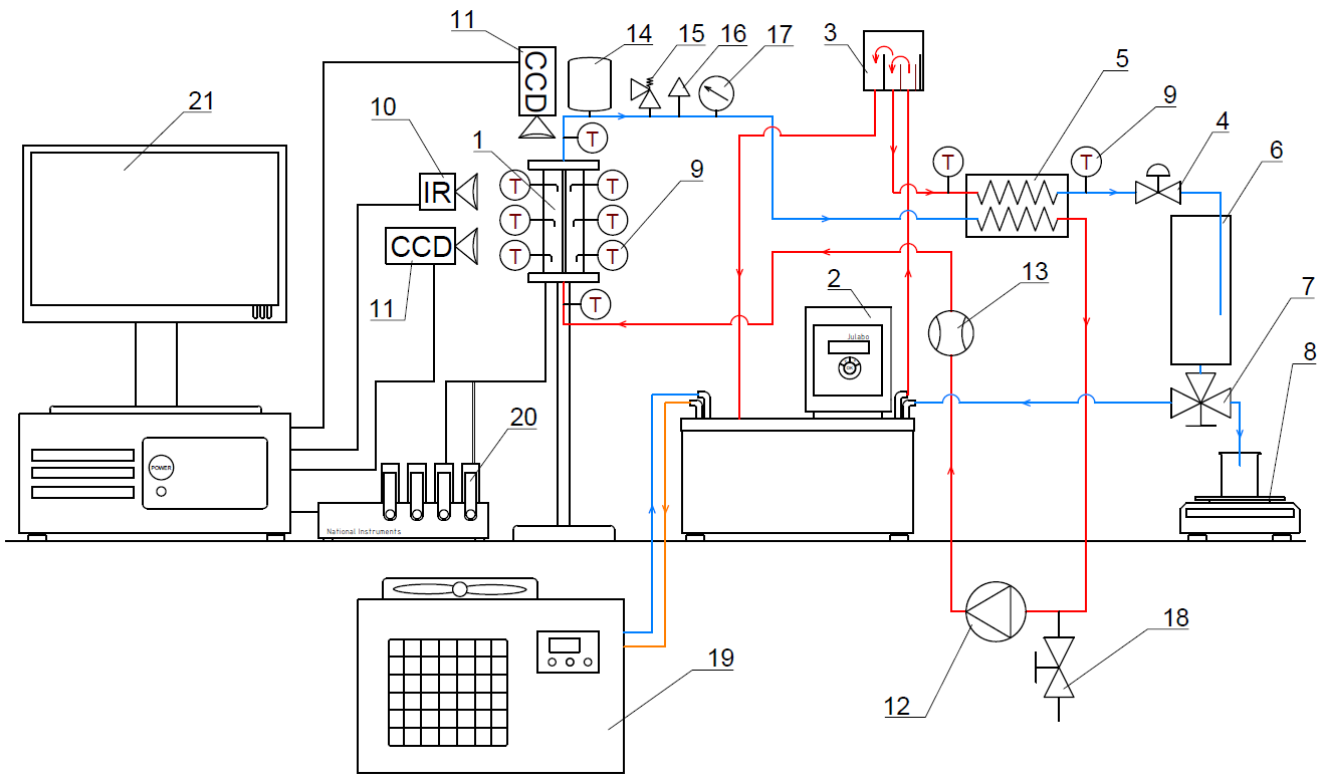


Figure 1 Scheme of the test section of the heat storage tank filled with PCM: 1 – experimental module with replaceable working element, 2 – heating thermostat with cooling coil, 3 – overflow vessel, 4 – control valve, 5 – plate heat exchanger, 6 – collecting vessel, 7 – three-way valve, 8 – precision balance, 9 – temperature sensor, 10 – thermal imaging camera, 11 – quick pictures camera, 12 – gear pump, 13 – water meter, 14 – diaphragm vessel, 15 – safety valve, 16 – automatic air vent, 17 – control pressure gauge, 18 – ball valve, 19 – industrial chiller, 20 – data acquisition system, 21 – computer

The measuring section consists of two circuits: primary and secondary, between which heat is transferred in a plate heat exchanger (5). The primary circuit has been designed for obtaining the largest possible temperature difference between the inlet and outlet of the heat exchanger (5), which will allow to determine the amount of transferred heat. The working fluid flow in this system is provided by a circulation pump built into the CORIO [JULABO] thermostat (2). The overflow vessel (3) equipped with a control valve enables to set flow on required level. Part of the liquid flows through the heat exchanger (5) and then to the collecting vessel (6), while the excess returns through the overflow channel to the thermostat bath (2). The collecting vessel (6) is equipped with a three-way valve (7).

In the normal position of the valve (7), the liquid after supplying / receiving heat in the heat exchanger (5) returns to the thermostat bath (2). The second position of the valve (7) allows working fluid to be redirected to the laboratory graduated cylinder located on the pan of the SBS-LW [STEINBERG] precision balance (8). By measuring the time and mass of the liquid, it will be possible to determine flow of the working fluid flowing in the primary circuit. Temperature of the working fluid at the inlet and outlet of the heat exchanger primary circuit site is measured by Pt100 (class A, 4-wire) resistance sensors. Task of the secondary circuit is to supply or receive heat from the heat storage tank while maintaining the condition of a constant wall temperature of the working element (it is assumed to maintain the temperature difference between the inlet and outlet of the tube at 0.1 K). To maintain the constant wall temperature, it is required to obtain the highest possible fluid flow. This circuit consists of the KPER 63 K2 [VEM] gear pump (12) which pumps the liquid into the measuring module (1). A water meter (13) mounted in this circuit enables to control working fluid flow level. Fluid temperature at the inlet and outlet of the test module is measured by Pt100 (class A, 4-wire) resistance sensors. After passing through experimental module (1), working fluid goes to the safety group, equipped with a diaphragm vessel (14) (also acting as a tank), safety valve (15), automatic air vent (16) and control pressure gauge (17). Next the fluid flows through the heat exchanger (5) in which it is heated / cooled, depending on the implemented cycle.

In both circuits, the working fluid is distilled water. In the cycle, in which the PCM must be melted, the working fluid is heated by an electric heater mounted in thermostat (7). Temperature of the process is controlled by thermostat (7) electronic, precise temperature control system. In the cycle in which the PCM must be solidified, the industrial chiller (19), which is connected to the copper coil placed in the thermostat bath (7), cools the working fluid to the required temperature level.

All temperature sensors, i.e. sensors measuring the temperature distribution inside the heat storage tank (15 T-type thermocouples, and 4 class A, 4-wire Pt100 resistance sensors), sensors measuring temperature of the working fluid in primary circuit (2 class A, 4-wires Pt100 resistance sensors) and sensors measuring the temperature of the working fluid in the secondary circuit (2 class A, 4-wires Pt100 resistance sensors) are connected to the NI eDAQ-9189 [NATIONAL INSTRUMENTS] (20) data acquisition system equipped with two NI 9212 thermocouple modules (which allow to connect a total of 16 thermocouple sensors), and one module for NI 9216 resistance sensors enabling the connection of 8 Pt100 sensors. Data are sent to the PC computer (21) equipped with LabView [26] software. Simultaneously



to temperature measurements, the process will be monitored using one thermal imaging camera C3 [FLIR] (10) and two cameras for taking quick pictures UI-1220ME-C-HQ [IDS] (11). Data from all cameras will be recorded on the computer set (21).

2.2 Description of experimental module

Figure 2 shows the 3D project of the demountable thermal module (a) and view of completed module (b).

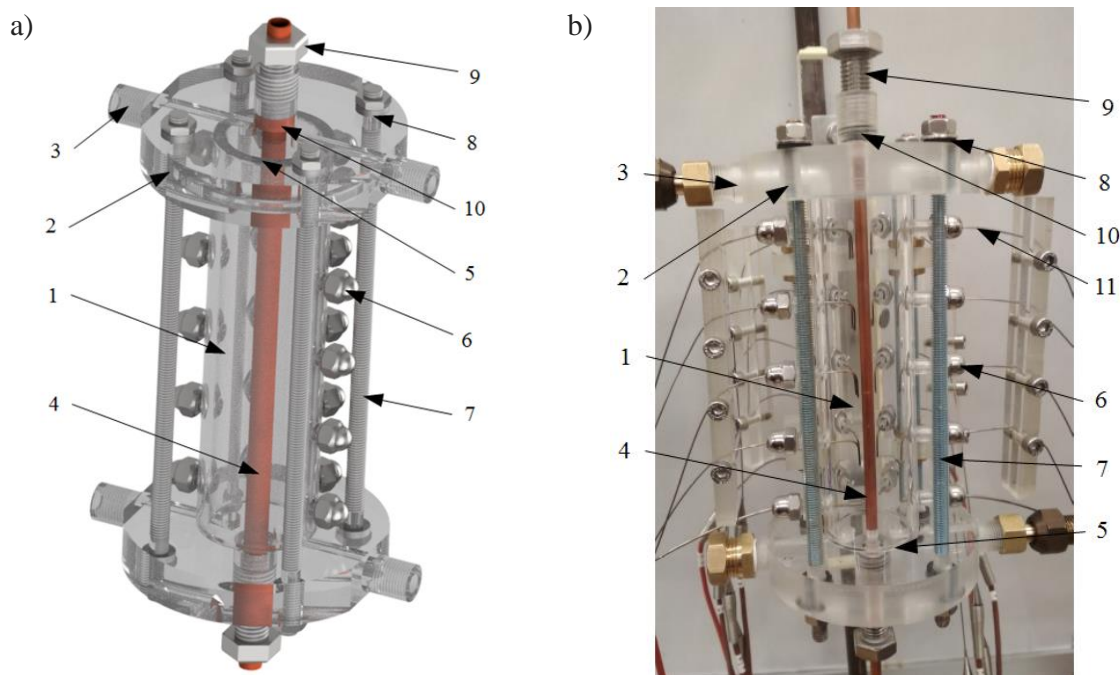


Figure 2 View of the experimental module: a.) 3D model; b.) real view: 1 – jacket; 2 – flanges; 3 – stubs; 4 – replaceable working element; 5 – rubber gasket; 6 – temperature sensors glands; 7 – threaded steel rods; 8 – rubber pads; 9 – working element glands; 10 – rubber gasket, 11 – temperature sensors,

The construction of the demountable version of the test module for studying the heat storage process using phase-change materials was aimed at enabling the replacement of the heat supplying / receiving element, changing the position of temperature sensors if necessary to change the measured plane, and to simplify cleaning of the module. The designed vessel consists of a jacket (1) made of PMMA pipe with an external diameter of 50 mm and an internal diameter of 40 mm. The jacket height is 169 mm, which after deducting the depth of the locating grooves made in the flanges (2) (3 mm on each side, where 1 mm occupies the seal) gives 165 mm of the active length of the module. The working element (4) is cooper tube with outside diameter equal to 10 mm and wall thickness equal to 1 mm. Thermocouple glands (6) fixing the position of the temperature sensors are glued to the jacket. This way of mounting sensors allows to change the radius on which the sensor is located, and also to

replace it in the case of a sensor failure. The closing elements of the vessel are flanges (2) made from PMMA, with 110 mm diameter and 20 mm thickness. Two conduits with a diameter of 8 mm were made in each flange to fill / empty the tank and clean it. The conduits are ended with 3/8" connection stubs (3). In the axis of the flanges, glands are used to seal the working element (6). A rubber gasket (10) was made as the pipe sealing element. This seal design ensures that the heat supplying / receiving element can move, which compensates for the change in the length of the elements associated with the materials thermal expansion. The flanges and jacket were mounted together by using four M8 threaded steel rods (7) and appropriate nuts and washers. Also additional rubber pads (8) were used to compensate thermal expansion of the module materials. The flat rubber gaskets (5) with the thickness 1 mm were used as a sealing between the flanges and the jacket. The working element that supplies / receives heat (4) is a tube made of copper with a 10 mm outer diameter and 1 mm wall thickness. To measure the temperature inside the experimental module next sensors were used: 15 T-type thermocouples with a 1 mm jacket diameter and a 300 mm length; 4 resistance sensors of the type Pt100, class A (4-wire) with a 1,5 mm jacket diameter and a 150 mm length of 150. In order to minimize measurement errors, thermocouple sensors, after placing them in the module jacket, were bent at a certain radius. To ensure repeatability of the sensor bending geometry, a special device was made, equipped with a hole with a diameter of 1 mm and a depth of 10 mm, in which the sensor is placed, ended with a cutting of a circle with a radius of 4 mm. Figure 3 shows the sensor geometry after bending and picture of the bended sensor.

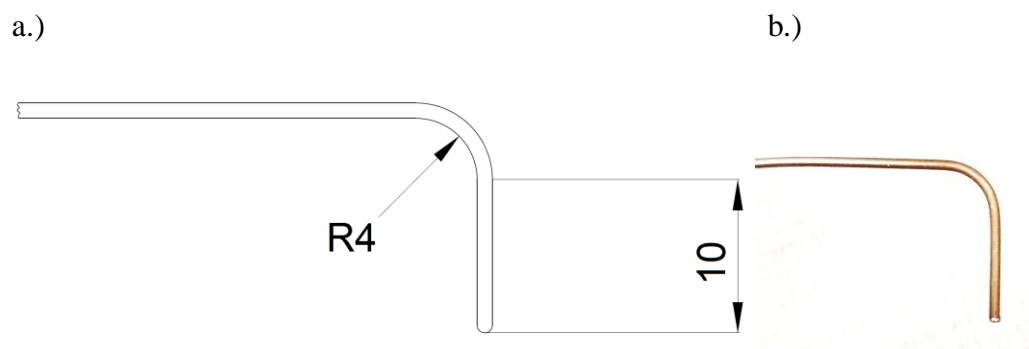


Figure 3. View of bended thermocouple sensor: a) geometry of the sensor; b) picture of the bended sensor

The sensors were arranged on 4 planes, placed relative to each other every 60°, 5 sensors in each plane. Sensors belonging to specific planes are covered on 4 different radius. Along the axis of the module, ends of sensors are placed on 5 surfaces, called respectively S1, S2, S3, S4, S5. Figure 4 shows the geometry of the sensor arrangement:

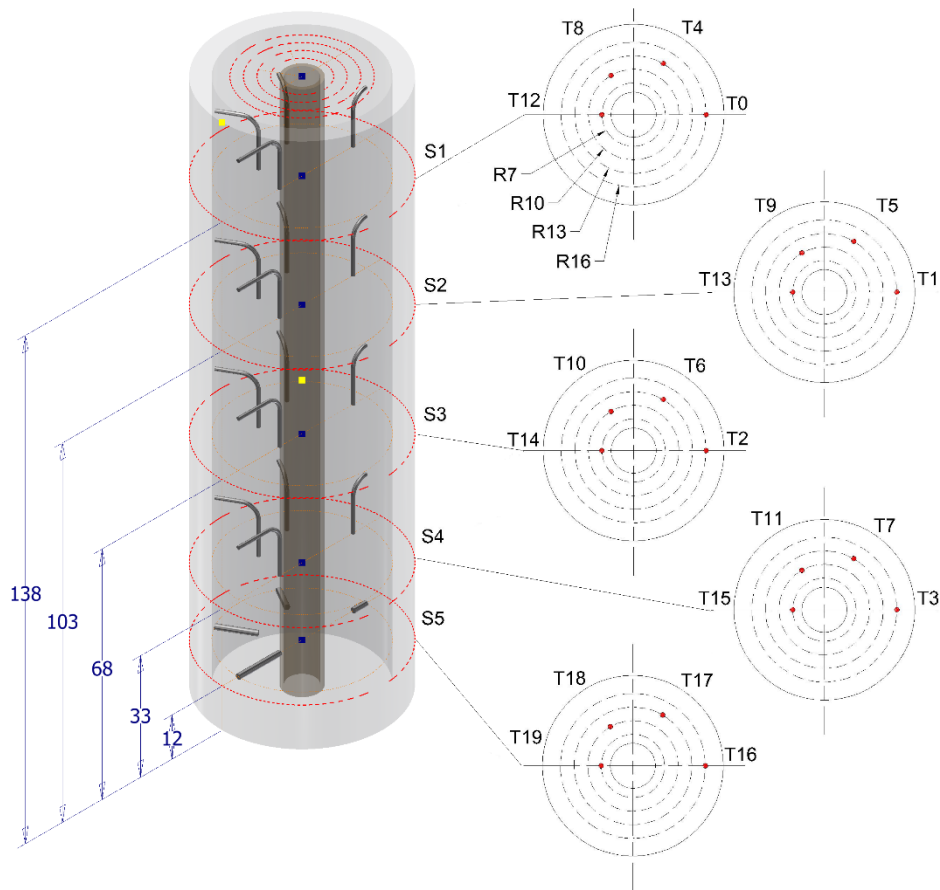


Figure 4 Arrangement of temperature sensors inside experimental module

Summarizing it should be noted that One of the distinguishing features of this experimental module is its modularity. As have been mentioned already in the article, the construction of the experimental module is demountable. It has been aimed at enabling the replacement of the heat supplying / receiving element, changing the position of temperature sensors if necessary to change the measured plane, and to simplify cleaning of the module. What is more in experimental module two conduits with a diameter of 8 mm were made in each flange to fill / empty the tank and clean it. This conduits have been using during calibration of temperature sensors mounted in the experimental module and each time during filling/emptying process of PCM. All module elements have been made form PMMA witch is a good isolator (conductivity less than 0,2 W/mK) and has a high light transmittance higher than 90%. What is more this material has a very good cutting properties, good chemical resistance and resistance for UV. Thanks using of PMMA it could be possible to observation of the change in the melting / solidification front both in the lateral and transverse planes. Due to used of special temperature sensors glands it have been possible to mounted them after bending process. Such an operation allowed for the placement of the thermocouple junction together

with the lead-in section of the sensor along the expected isothermal lines. This approach follows the experimental procedures found in the literature [27].

2.3 Description of experimental procedure

The measuring cycle begins with the solidification of the phase change material. In order to prepare PCM at a uniform temperature, the appropriate amount of material placed in the graduated cylinder is heated to 35°C using an electric heater equipped with an electromagnetic stirrer. At the same time, to cool the module, a working fluid with a temperature of 17°C is passed through the working element. This process is carried out until all temperatures inside the module are equalized. The amount of working fluid flowing through the primary system is also adjusted. Then, the phase change material is placed in an indirect vessel, the design of which allows it to be attached to one of the measuring module connection stubs. At the top of the indirect vessel valve is placed to which a compressed nitrogen is connected. On the opposite stub, an overflow pipe is attached. After starting the measurement program and recording images from cameras, first the valve placed between the measuring module and the indirect vessel is opened, then by exerting the minimum pressure, the module is filled with phase change material. After de-aeration of the module, valves on both connectors are closed. The use of this procedure allows achieving a uniform PCM initial temperature (± 0.5 K) at all points. During the experiment, temperatures inside the PCM, working fluid (water) at the inlet and outlet, heat exchanger inlet and outlet at the primary system side are measured simultaneously. Every 30 minutes the mass flow of the liquid flowing in the primary system is measured. This is done by redirecting the flow of liquid to the measuring cylinder placed on the balance where mass of liquid is measured, and by measuring the filling time with a stopwatch.

After completing the PCM solidification cycle, the system is prepared for performing the melting cycle. For this purpose, the supply of working liquid to the measuring module is cut off by using a bypass, and the medium flowing through the rest of the system is heated to 37°C. A correspondingly higher temperature level during system heating is required to ensure that the temperature level is maintained at 33°C during the melting process, which was determined during system calibration. After the system temperature is established, the liquid flow through the working element is opened, which begins the melting process of the PCM. In the next steps of cycle measurements are carried out in the same way as during the solidification process. All experiments have been carried out for constant wall temperature. The wall constant temperature has been preserved by large amount of water flowing through



the heat transfer surface. The heat capacity of thermostatic bath has been enough that the temperature differences between the inlet and outlet to the heat supply / receiver element could be neglected. What is more as a working element has been choose cooper tube with wall thickness 0.5 mm, for that fact the wall thermal resistance could be neglected and the wall temperature assumed as equal to water temperature.

To minimize heat loss to the environment, all system components and tubing were insulated using polyurethane insulation, while the measuring module was insulated using wool. Approx. $\frac{1}{4}$ of the module jacket and part of the upper flange remained exposed to observe the process using a thermal imaging camera and high speed cameras.

2.4 Thermal performance analysis

The heat supplied / received from the phase change material can be calculated from energy balance of plate heat exchanger (see Fig 1) at primary circuit. As has been mentioned earlier The primary circuit has been designed for obtaining the largest possible temperature difference between the water inlet and outlet of the heat exchanger (5), which will allow to determine the temperature differences with relatively small uncertainty level. The experimental setup also allows to working fluid to be redirected to the laboratory graduated cylinder located on the pan of the SBS-LW [STEINBERG] precision balance. It is possible to precisely measure very small amount of flowing water and base on that it is possible to calculating mass flow of working fluid flows in primary circuit. Summary the heat flux can be found from equation:

$$\dot{Q} = \dot{m} \cdot c \cdot \Delta T \quad (1)$$

The average amount of released heat in solidification process (from the time point for the solidification process start- τ_1 to the moment when the PCM temperatures at the S1 surface are equal to subcooling temperature- τ_2).

$$Q_m = \frac{1}{\tau_m} \int_{\tau_1}^{\tau_2} \dot{m} \cdot c \cdot \Delta T \quad (2)$$

The average amount of absorbed heat in melting process (from the time point for the solidification process start- τ_1 to the moment when the PCM temperatures at the S5 surface are equal to melting temperature- τ_2).

$$Q_s = \frac{1}{\tau_s} \int_{\tau_1}^{\tau_2} \dot{m} \cdot c \cdot \Delta T \quad (3)$$

The average latent heat is equal:

$$h_{ls} = \frac{Q}{M_{PCM}} \quad (4)$$

Where Q is equal to amount of heat received/absorbed during solidification/melting process.

2.5 Phase change material characteristic

A coconut oil with melting temperature of 25°C was chosen as the PCM. Because of fact that this is natural , raw material this product may have slight differences in fats composition. In open literature it is not easy to found uniform thermophysical properties of that substance. One of the main issue is to evaluated latent heat of such substance. The literature data show varied results for that properties from 249 to 72 kJ/kg [28]. The results probably depending also on the type and accuracy of used equipment. Due to that fact the properties of coconut oil has been verified by authors. The latent heat has been estimated based on the energy balance of the experimental section. Ten tests were conducted of melting and solidification the material under the same conditions. The obtained values were averaged. Based on the results, the phase transition heat was assumed to be 178 kJ/kg. The thermal conductivity has been obtained from Tempos Thermal Properties Analyzer, for temperature range 17°C-30°C, with accuracy +/-10%. What is more for lowest temperature (17°C) also the volumetric specific heat capacity and diffusivity have been measured. Those two values could not been obtained for higher temperature range due to the equipment capability. Furthermore the dynamic viscosity has been experimentally obtained for temperature range 21 °C-40° C. In that test has been used Vpad rotation viscometer with accuracy +/-1%.

Due to the fact that especially thermally properties are crucial for properly physical model of melting solidification phenomena, that values have been determination based on a statistical sample. To determine of conductivity, volumetric specific heat capacity and diffusivity more than 45 measurements were carried out each time for the same substance temperature value. The measurements have been carried out by dual-needle sensor. According literature this kind

of measurements are sensitive for ambient factors like vibration due to e.g. HVAC systems working, PC working, personnel activity in lab [29,30]. That is why the measurements has been done at night without working HVAC system. Also the vertical position of probe have been carefully set to diminish free convection influence at the results. In case of latent heat has been determined directly from energy balance of test section. As has been emphasized earlier special construction of test section enabled determination of the amount of heat supplied to / received from the phase change material. This parameter has been determination also based on a statistical sample. To determine latent heat more than 50 cycles of solidification/melting have been carried out.

Tab. 1 Uncertainties of selected parameters.

Parameter	Operating range	Uncertainty
T_{PCM}	10°C -60°C	+/-0.3 K
T_w	10°C -60°C	+/-0.05 K
\dot{m}_c	8,63-11,27 g/s	1,2%
M	260-360 g	+/-0,1g
\dot{Q}	0,1-6 W	+/-10 ⁻³ W
λ	0,25-0,7 W/mK	+/-10%
C_v	3,85 -2,25 MJ/m ³	+/-10%
a	0,02 -0,2 m ² /s	+/-10%
μ	25 -550 mPas	+1 %
ρ	920-950 kg/m ³	+/-10,9%

All sensors in measurement system have been check after their mounted into experimental module. In experimental module two conduits with a diameter of 8 mm were made in each flange to fill / empty the tank and clean it. This conduits have been used to fill the module by thermostatic bath. The water inlet/outlet temperature have been check during the calibration. The difference between the inlet / outlet temperature was not more than +/- 0.05 K (see Figure 5).

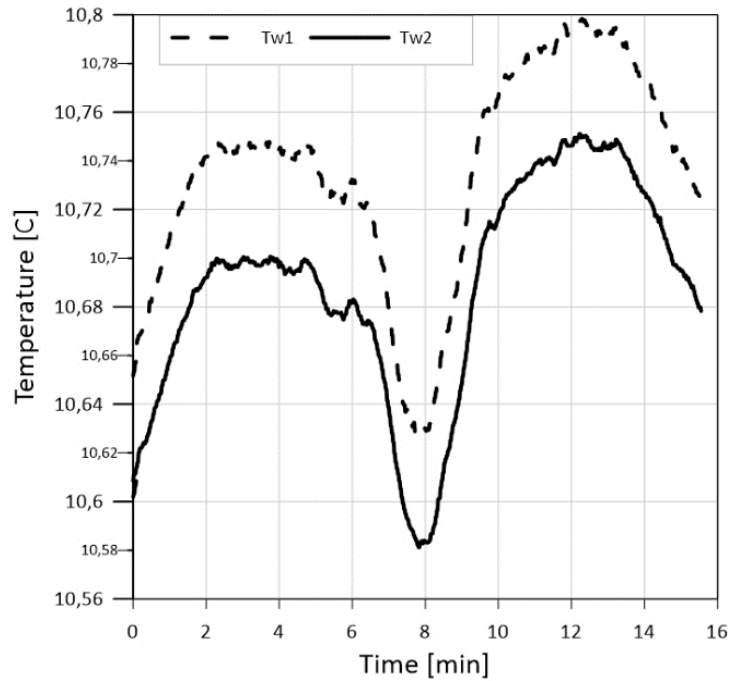


Figure 5 Temperature of water inside measurement module during calibration

The calibration have been made for temperature range 10 °C to 40° C., the example of results has shown at Figure 6. To minimize so call fin effect of thermocouples and the influences of ambient at the temperature measurements all thermocouple have been bend. Such an operation allowed for the placement of the thermocouple junction together with the lead-in section of the sensor along the expected isothermal lines. This approach follows the experimental procedures found in the literature [27].

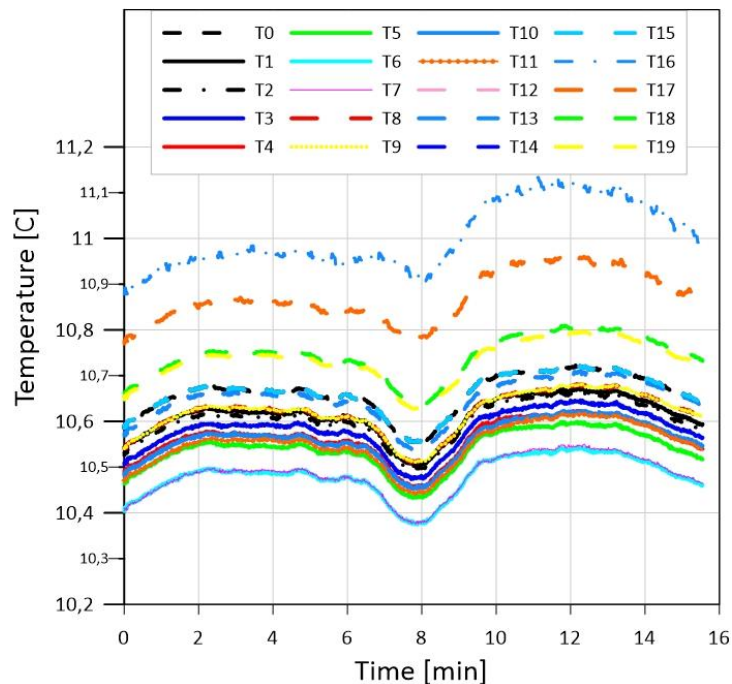


Figure 6 Selected results of temperature measurements during calibrations

However at the bottom surface there was no chance to use dented thermocouples due to limited space. The temperature points from T16 to T19 have been measured by resistance sensors (PT-100) with first class. The experimental results have shown that those sensors had the biggest temperature differences during calibration procedure. The temperature difference for thermocouple was not larger than $\pm 0,1$ K, however for resistance sensors was equal to $\pm 0,3$ K. Finally the uncertainty for temperature sensors inside PCM has been set assumed as $\pm 0,3$ K. The uncertainty for water temperature sensor have been assumed as $\pm 0,05$ K.

3. Experimental investigation results for melting/solidification process

3.1 Melting process

As it is well known from open literature coconut oil is a mixture of fatty acids: Caproic acid (0.2%-0.5%), Caprylic acid (5.4%-9.5%), Capric acid (4.5%-9.7%), Lauric acid (44.1%-51%), Myristic acid (13.1%-18.5%), Palmitic acid (7.5%-10.5%), Stearic acid (1.0%-3.2%), Arachidic acid (0.2%-1.5%), Oleic acid (5.0%-8.2%), Linoleic acid (1.0%-2.6%) [31]. The melting process for pure substance is characterized by constant melting temperature for particular pressure. However for mixture of substances usually do not display a sharp melting point, they melt over a range of temperatures, see Figure 7. It seems to better talk about the conception of appearance melting temperature rather than melting temperature like in case of pure substances. It should be also noted that for mixtures the appearance of melting temperature is lower than melting temperature of compounds forming the mixture [32]. Furthermore generally the melting process is more complex for mixture substance than the pure, single compound substance.



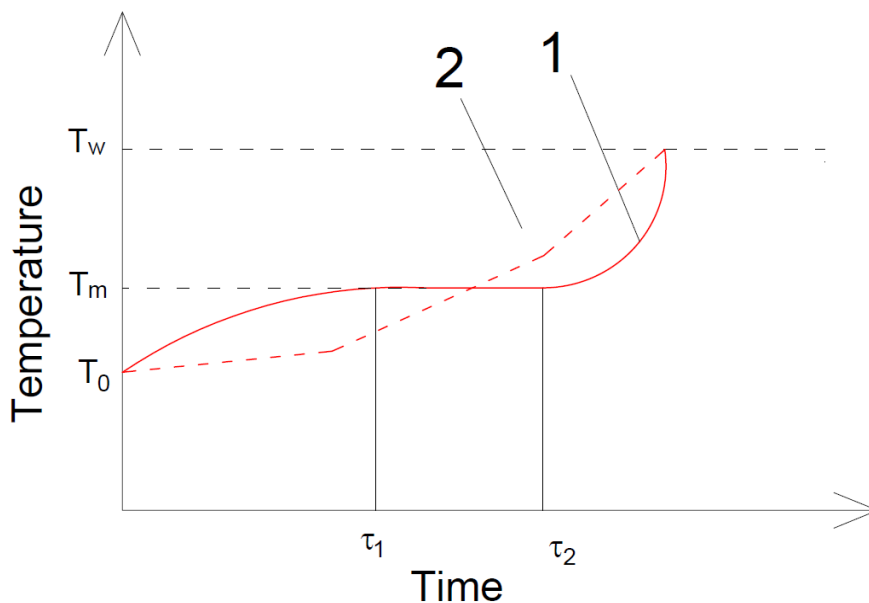


Figure 7 Theoretical temperature distributions for the PCM melting process: 1- temperature characteristic for pure substance, 2 – temperature characteristic for mixture substances, T_0 - initiation temperature of heating process, T_m - melting temperature, T_w - wall temperature, τ_1 - time point for the melting process start, τ_2 - point time for the end of the melting process

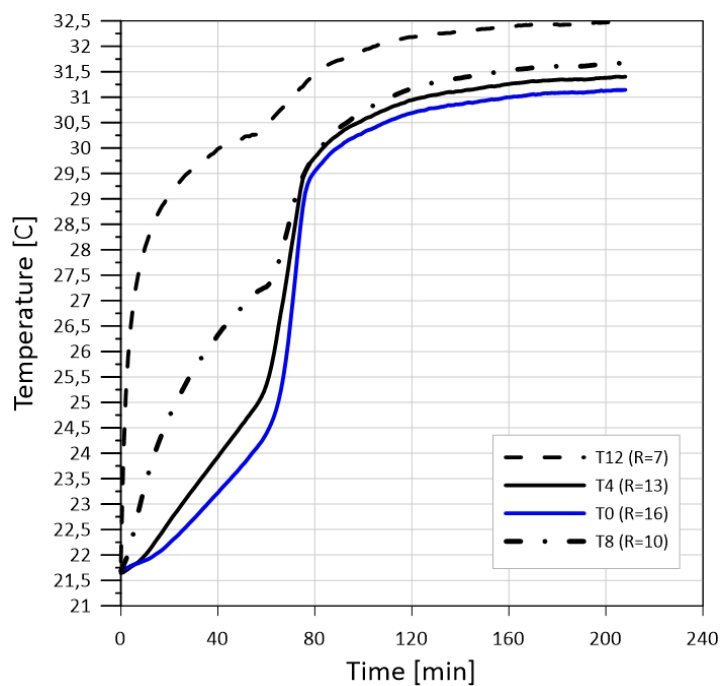


Figure 8 Temperature profile evolution as a function of the radial position during melting process with constant wall temperature condition ($T_s=33^\circ\text{C}$) on surface S1



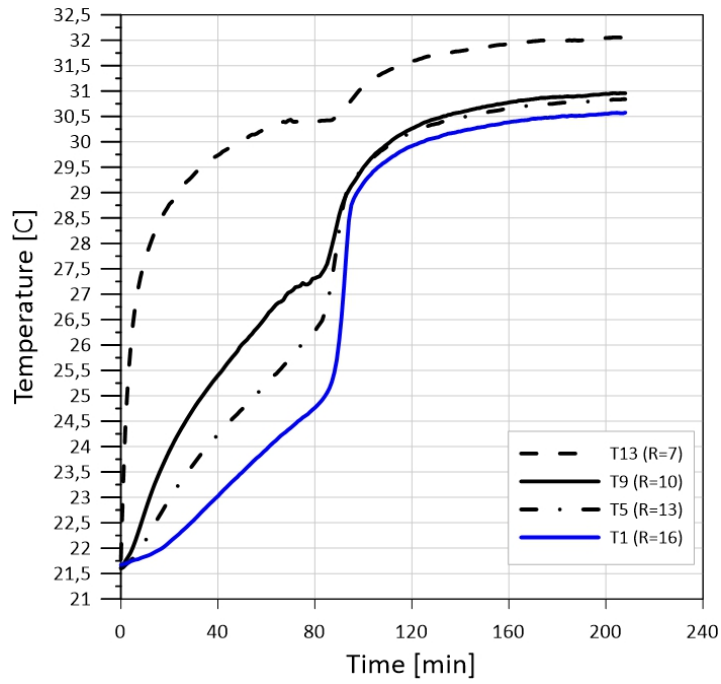


Figure 9 Temperature profile evolution as a function of the radial position during melting process with constant wall temperature condition ($T_s=33^\circ\text{C}$) on surface S2

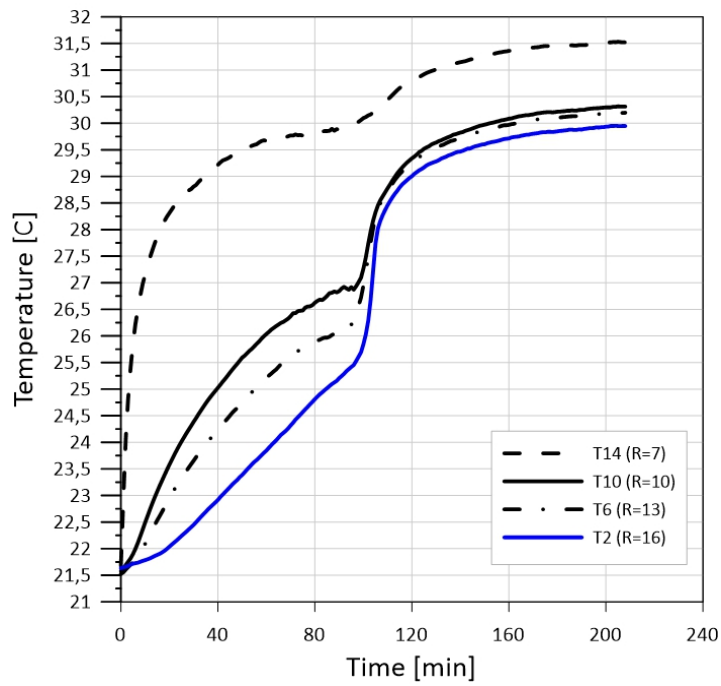


Figure 10 Temperature profile evolution as a function of the radial position during melting process with constant wall temperature condition ($T_s=33^\circ\text{C}$) on surface S3

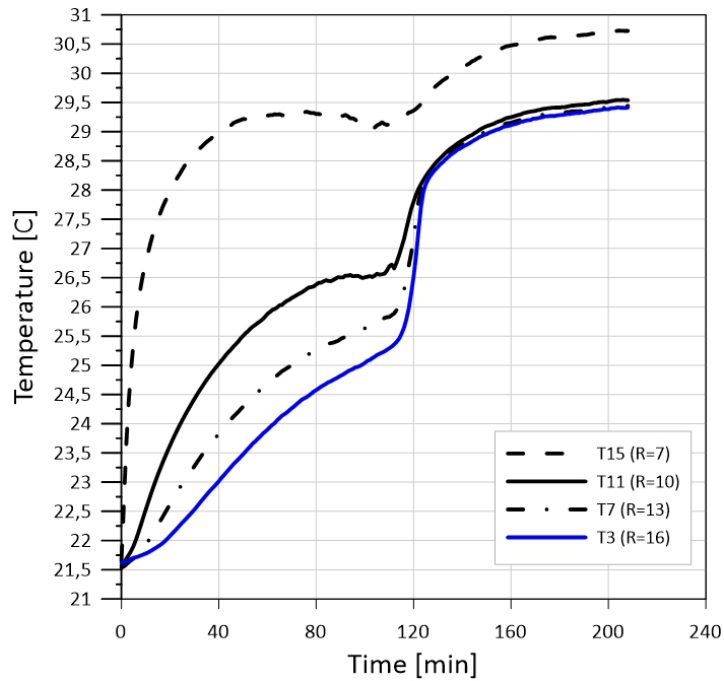


Figure 11 Temperature profile evolution as a function of the radial position during melting process with constant wall temperature condition ($T_s=33^\circ\text{C}$) on surface S4

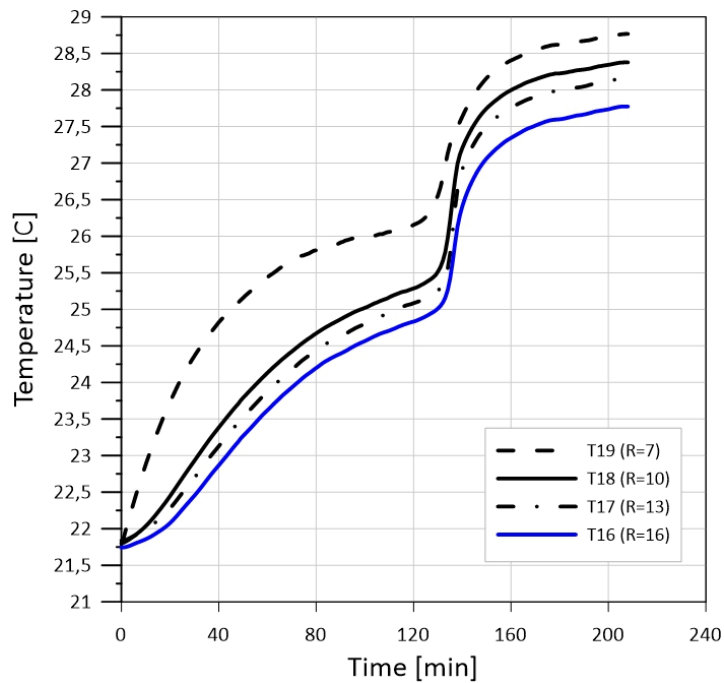


Figure 12 Temperature profile evolution as a function of the radial position during melting process with constant wall temperature condition ($T_s=33^\circ\text{C}$) on surface S5

Analyzing the results for melting of coconut oil it is clearly seen that the same cross-section surface the end of melting appearance in the same time point. What is more the time of melting decrease with increase the distance from heat transfer surface. There is also clearly to observe the difference level of appearance melting temperature in the radial direction. It could be explained by the fact of thermal resistance growth with growing the radial distance from wall of the tube (heat source). The highest temperature level is reached for sensors located

closest to heat transfer area. In this region it has been observed sharp temperature rise. With the growing radial distance from heat transfer surface the growth rate of temperature decrease. Nevertheless for that fact, for all temperature profiles could be observed the same stages. At first stage temperature undergoes a stable increase. In this stage there is clearly domination of heat conduction mechanism. The next stage is characterized by smooth temperature growing. During this time period the material is melting and absorbing latent heat. That period end by sudden rise of temperature. It could be explained by the convective flow in the liquid phase of working fluid. After that it could be observed slowly temperature rise until the heat source temperature is reached. It should be also noted the appearance of thermal stratification effect. This is due to the fact that at the beginning of process first is melts a thin layer close to inner tube from the top to the bottom . It is mean that this process is strongly influences by natural convection effect. Hot fluid is displaced from the top to the bottom of cylinder. Circulation of liquid phase more effectively accelerate melting process at the top part of cylinder compare to the bottom one. This is effect of larger temperature differences between the liquid and solid materials at upper part of cylinder. Regarding that fact it could be noted that natural convection accelerate the heat transfer in the upper region of cylinder and weakens the heat transfer in the bottom one. The similar conclusion have been deduced in many studies form the literature [33].

3.2 Solidification process

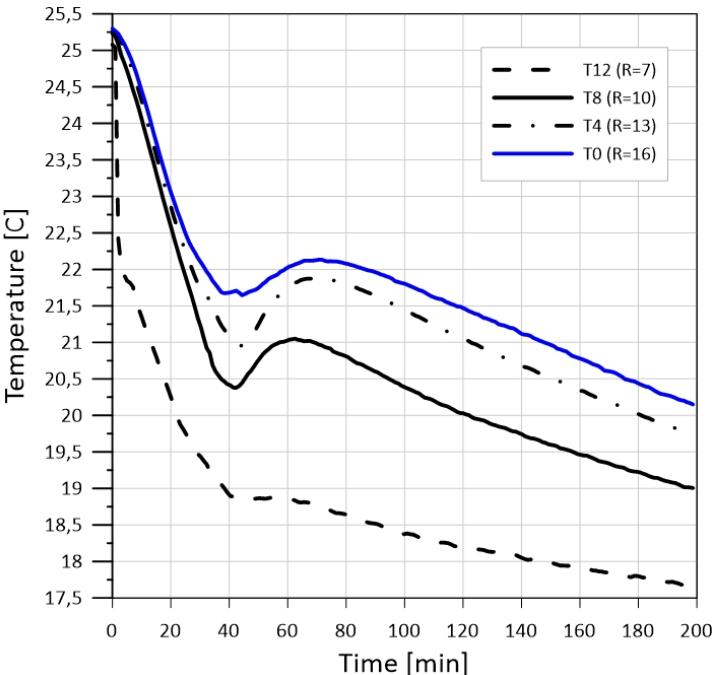


Figure 13 Temperature profile evolution as a function of the radial position during solidification process with constant wall temperature condition ($T_s=17^\circ\text{C}$) on surface S1

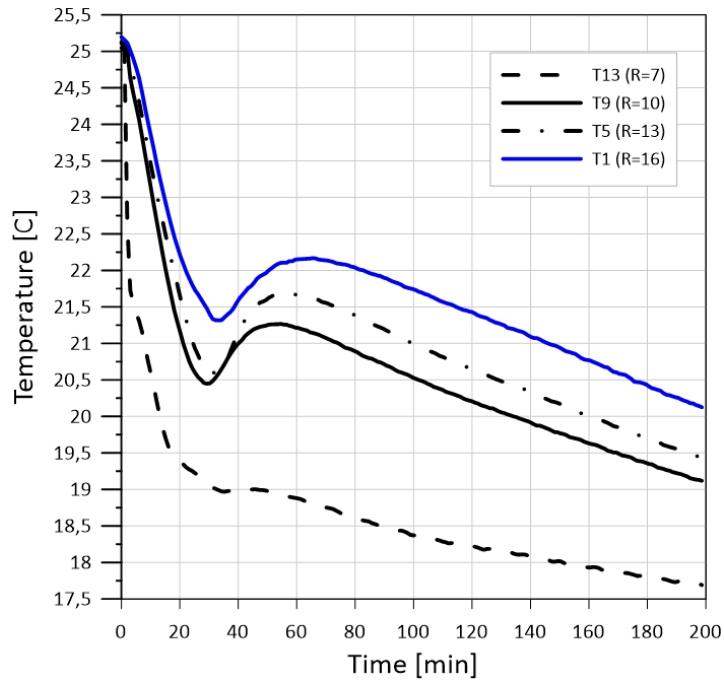


Figure 14 Temperature profile evolution as a function of the radial position during solidification process with constant wall temperature condition ($T_s=17^\circ\text{C}$) on surface S2

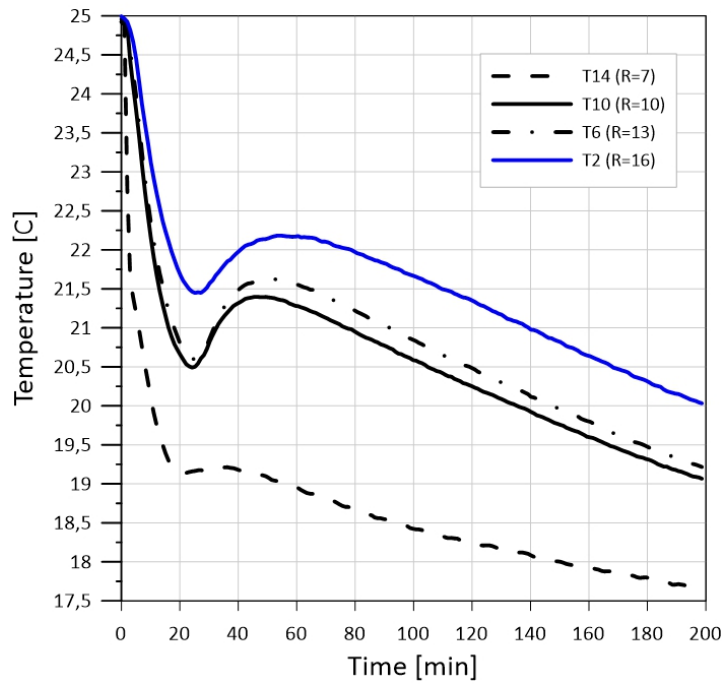


Figure 15 Temperature profile evolution as a function of the radial position during solidification process with constant wall temperature condition ($T_s=17^\circ\text{C}$) on surface S3

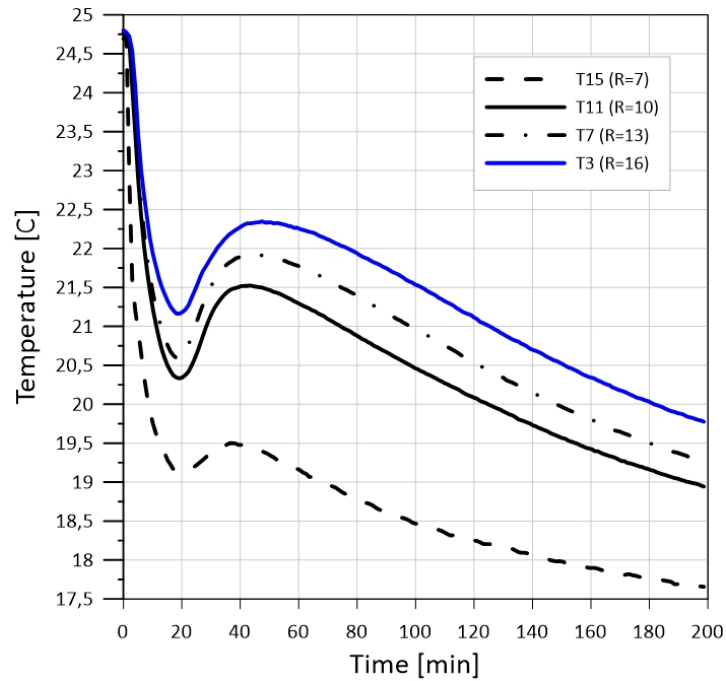


Figure 16 Temperature profile evolution as a function of the radial position during solidification process with constant wall temperature condition ($T_s=17^\circ\text{C}$) on surface S4

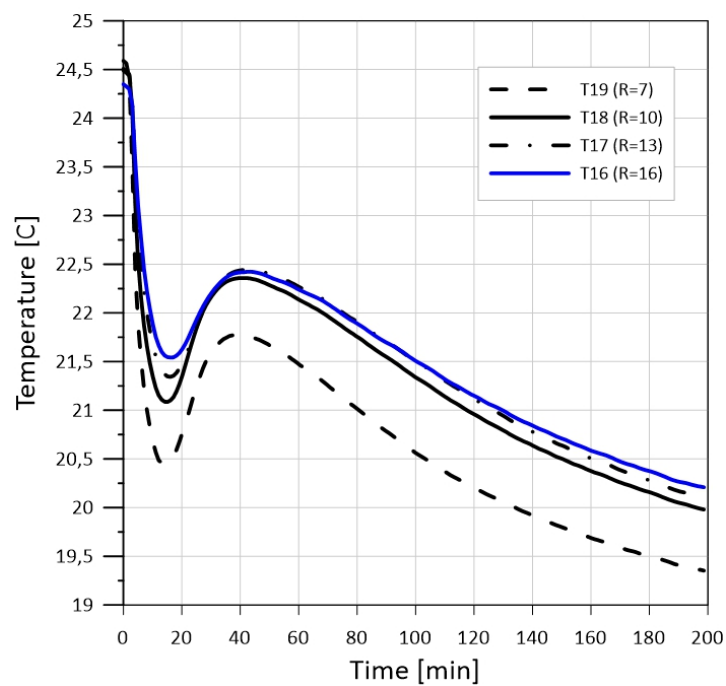


Figure 17 Temperature profile evolution as a function of the radial position during solidification process with constant wall temperature condition ($T_s=17^\circ\text{C}$) on surface S5

The temperature profiles recorded versus time have been clearly shown the appearance of sub cooling phenomena during cooling process of PCM. It could be observed characteristic (constant) time point of appearance of sub cooling temperature for the same cross-section surface of cylinder. It is an evidence that the PCM commenced the nucleation process

at the same time. The significant observation is also that the time span of the plateau during the phase change increased with the growing radial distance from heat transfer surface. The similar observation can be found in experimental studies from the literature [34]. The presented results shown similar stages of the solidification process, see Figure 18. However similar to melting process, in the radial direction there have been not observed the same phase change temperature. What is more the sub cooling temperature were different. The lowest phase change and subcooling temperatures level is reached for sensors located closest to heat transfer surface.

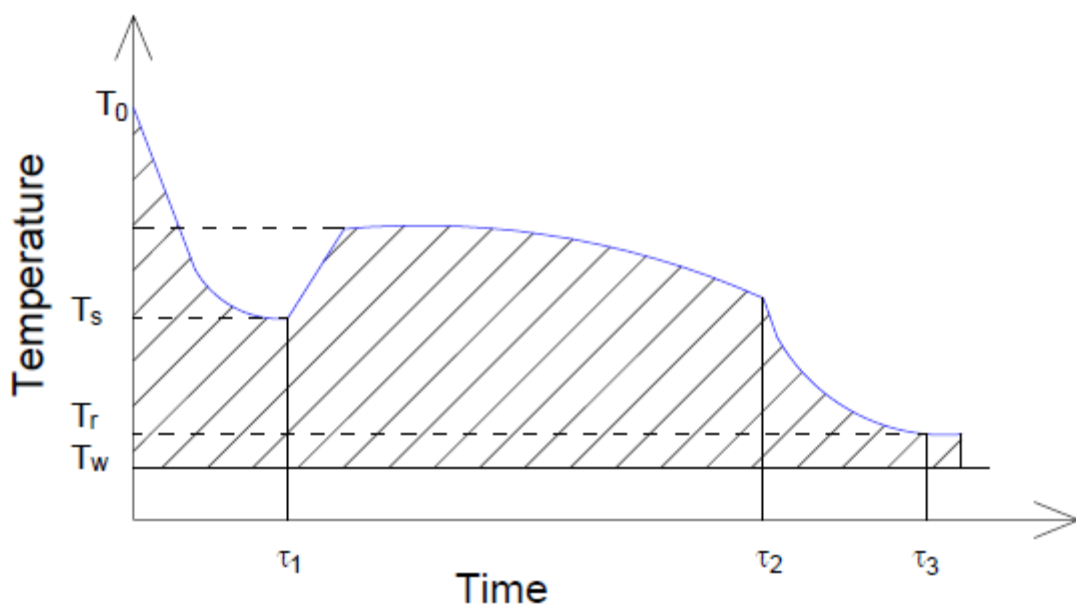


Figure 18 Theoretical temperature distributions for the PCM solidification process: T_0 - initiation temperature of cooling process, T_m - solidification temperature, T_s - subcooling temperature, T_r - end cooling process temperature, T_w - wall temperature, τ_1 - time point for the solidification process start, τ_2 - point time for the end of the solidification process, τ_3 - time point for the end of the cooling process

3.3 Visual observations

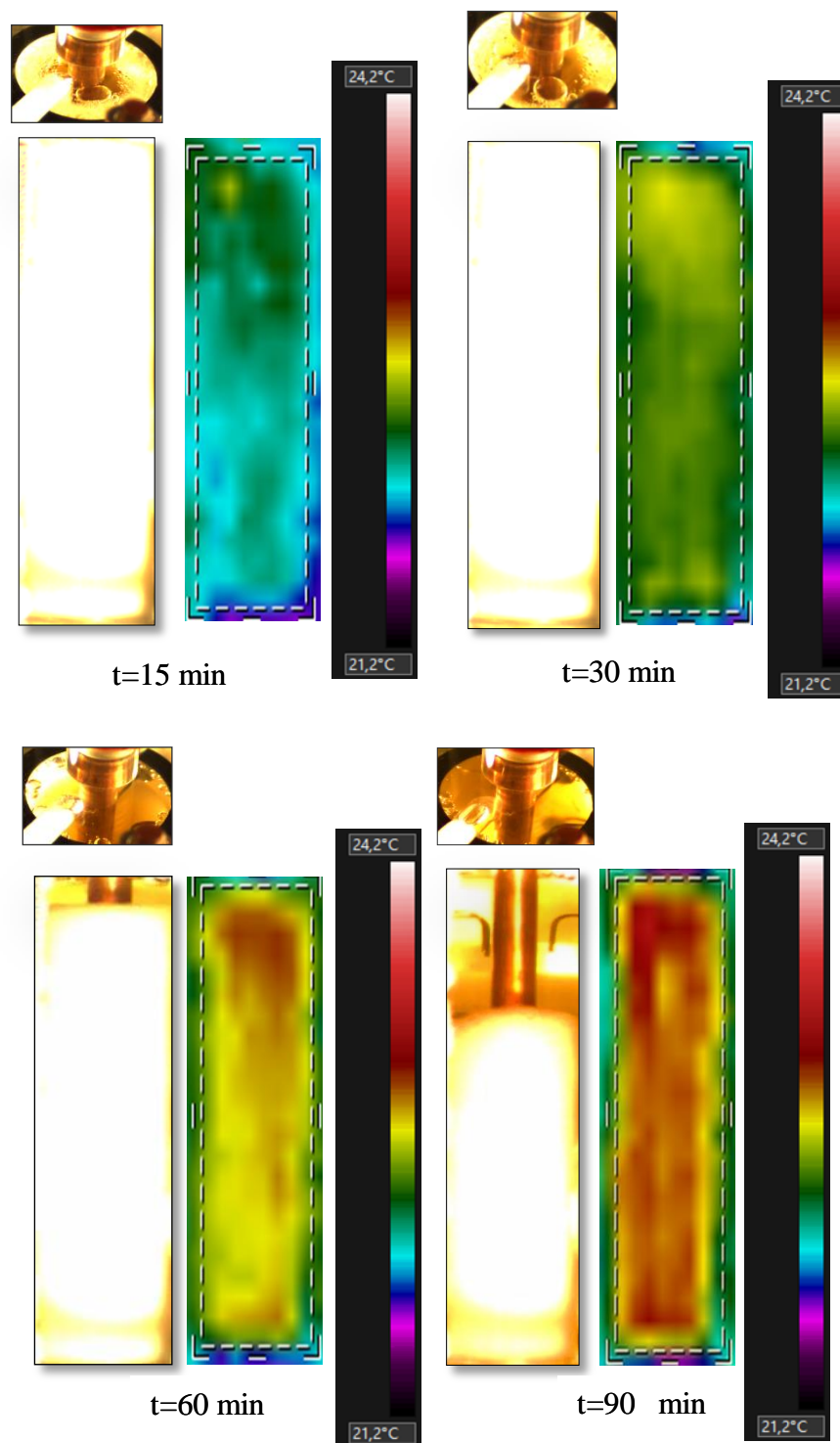


Figure 19 Visualization of melting phenomena: melting front photos for lateral and frontal surfaces and the frontal surface infrared photos

It should be highlighted that natural convection causes the non-uniform solid–liquid interface and temperature distribution in axial direction [13]. The shape of solid–liquid interface during

the melting process had been recorded by two analogy cameras and infrared camera. At the same time observation have been carried out for frontal as well as lateral surface. In the first melting stage appears only thin layer of liquid close to heat transfer surface. What is more that layer is thicker at the top of tank compare to layer at the bottom one. It is clearly evidence of strong influence of natural convection phenomena at the melting process. The infrared photos of lateral surfaces clearly confirmed significant influences of natural convection for melting processes of PCM. The temperature stratification is drop with increasing of amount of liquid fraction in the experimental module. Circulation of liquid phase more effectively accelerate melting process at the top part of cylinder compare to the bottom one. The temperature field is more uniform in the areas of conduction mechanism domination. That areas has been located near outer/lower regions of tank. Even if the PCM layer seems to be very thin close to the edge of the tank , in those places PCM remains solid for large operating times. It could be explained by the fact that the amount of heat transferred to PCM at these conditions is not sufficient to achieve complete melting. The shape of solid–liquid interface seems forms an inverted truncated cone. The liquid layer at the top of tank expands in radial direction till the moment to reach boundaries of tank. From that stage liquid phase begins to move not only in the vertical direction but also circulates along the radius of solid–liquid interface. The process visualization has been presented at the Figure 20.

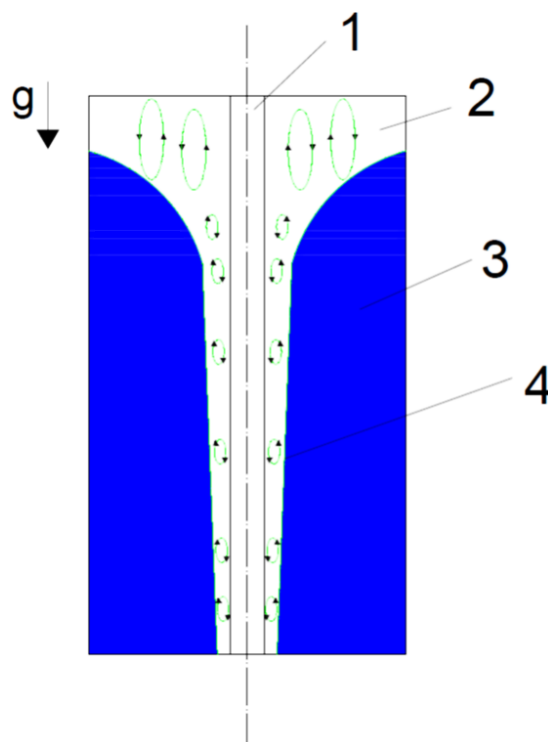


Figure 20 Physical interpretation of melting phenomenon in vertical cylinder configuration: 1- working channel, 2 - liquid phase, 3- solid phase , 4- phase separation surface

The shape of solid–liquid interface during the solidification as well as in melting case process had been also recorded by two analogy cameras and infrared camera. At the same time observation have been carried out for frontal as well as lateral surface, see Figure 21.

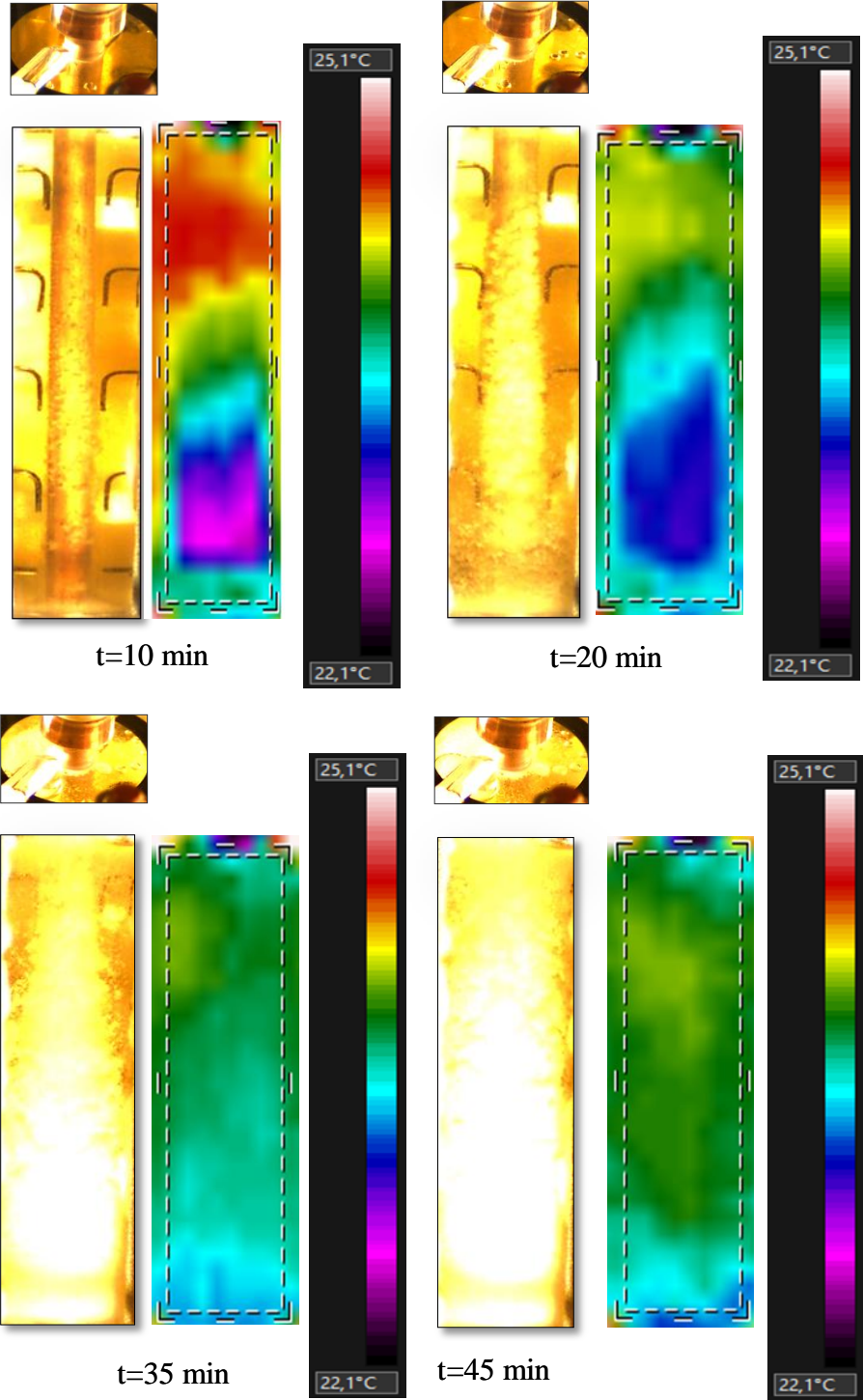


Figure 21 Visualization of solidification phenomena: solidification front photos for lateral and frontal surfaces and the frontal surface infrared photos

In the first solidification stage appears only thin layer of solid phase close to heat transfer surface. It could be also observed that at the same time, the solid phase sinks to the bottom of the tank. It could be explained that the solid phase detaches from the surface of the channel and falls under the influence of gravity. However it is seems that solid phase is also created at nucleation sites in the whole volume of substance. What is more solid layer is thicker at the bottom of the tank compared the top. It is clearly an evidence of natural convection phenomena also at the solidification process. However this influence decreases with increasing solid phase content. The infrared photos of lateral surface have been shown, like in case of melting process, the temperature stratification . At the beginning of process , several temperature layers are visible in the volume of the reservoir. The temperature stratification, however reduce quickly due to increasing domination of conduction heat transfer mechanism. That domination is very fast especially in the areas located near lower regions of tank and the heat transfer surfaces. The temperature difference between top and the bottom part of tank is decreased with increase of amount of solid phase in the volume of reservoir.

At the beginning of the solidification process the shape of solid–liquid interface seems forms an truncated cone, it seems like mirror image to the shape observed during melting process. The solid layer at the bottom of tank expands in radial direction till the moment it reaches boundaries of the tank. From that stage solid phase begins to increase not only in the radius but also at the vertical direction. It is clearly to observed mushy zone. The process visualization has been presented at the Figure 22.

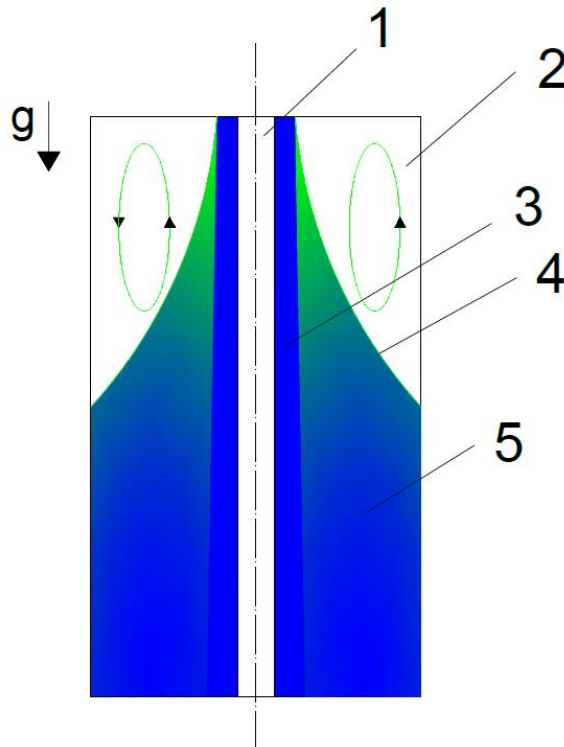


Figure 22 Physical interpretation of solidification phenomenon in vertical cylinder configuration: 1- working channel, 2 - liquid phase, 3- solid phase , 4- phase separation surface, 5- mushy zone (solid+liquid phase)

4. Analysis

The goal of this analysis was to provide a simple method to predict presented module with the charging/discharging system. This simple approach is of great value during the early design stage because it allows the designer to simply evaluate the influence of the latent TES functionality on the overall system performance in an integrated manner based on minimal input parameters of the latent TES.

The modeling of the heat stored or released in the PCM was achieved by using a constant heat resistance R_{th} of the module for both melting and solidification process. The energy balance in the volume considers the change of PCM temperature, modeled as point mass. Therefore the governing energy equation for the PCM yields:

$$M \cdot c(T) \cdot \frac{dT}{d\tau} = -\frac{1}{R_{th}} (T - T_w) \quad (1)$$

Due to the latent heat of phase change the specific heat was modified to incorporate it [35], the value of latent heat was assumed as $h_{ls}=178 \text{ kJ/kg}$. The apparent specific heat is a function of latent and sensible heat:

$$c(T) = \frac{c_p dT + h_{ls} \cdot F^*}{dT} \quad (2)$$

In order to avoid the discontinuity and simplify the natural mixture properties it was found that the latent heat can be distributed with Gaussian function, according to eq.3.

$$F^* = \frac{1}{\sigma \cdot \sqrt{2 \cdot \pi}} e^{\left(-\frac{1}{2} \left(\frac{T - T_{ls}}{\sigma} \right)^2 \right)} \quad (3)$$

Resulting apparent heat is presented in Figure 23. In further analysis both the thermal resistance R and apparent heat distribution $c = f(\sigma)$ was analyzed. The analyses were performed with Eulerian approach Octave [36].

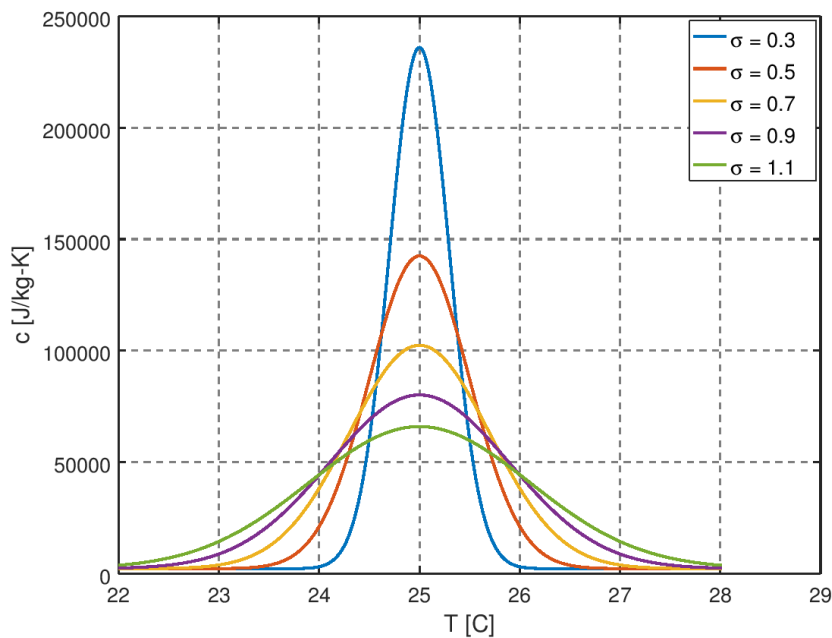


Figure 23 Apparent heat of the coconut oil modelled with eq.(2).

Experimentally obtained temperature and heat transfer distributions were compared with the simplified model. Figure 24 and Figure 25 presents calculated temperature evolution compared with experimental points obtained during melting process. Analogically presents calculated and experimental heat transfer in melting process. Based on the best fit approach the parameters R and σ were evaluated to be 1.3W/K and 1.1 respectively. The T_{ls} temperature was set as 25°C.

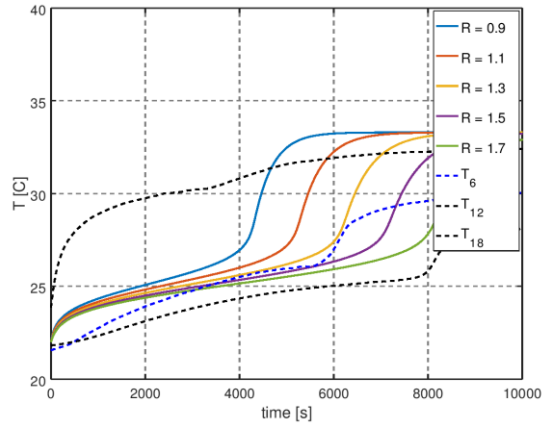


Figure 24 Melting process temperature for $\sigma = 1.1$

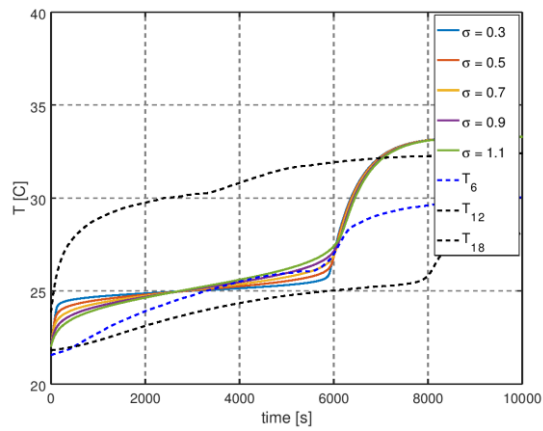


Figure 25 Melting process temperature for $R = 1.3 \text{ W/K}$

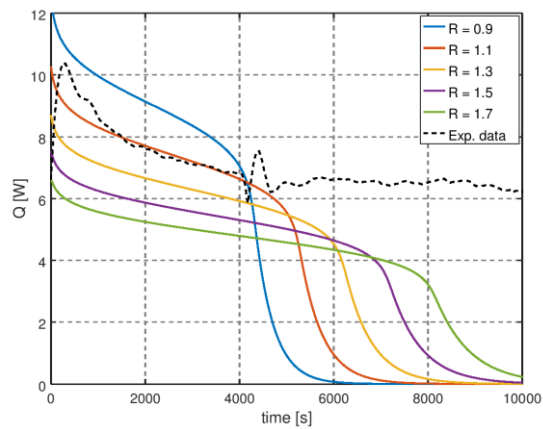


Figure 26 Melting process time dependent heat transfer for $\sigma = 1.1$

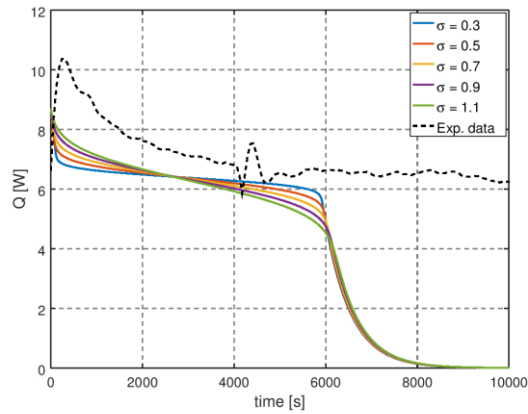


Figure 27 Melting process time dependent heat transfer for $R=1.3$ W/K

In the same manner the solidification process was evaluated as can be seen in Figs. 26 to 29. Surprisingly it was found that R and σ can be described identical as during melting process while the T_{ls} temperature was set as 21°C . One must remember that the Thermal resistance is a function of the temperature gradient due to the convection effects in the PCM volume. Therefore authors future works will be focused on the analyses of these effects.

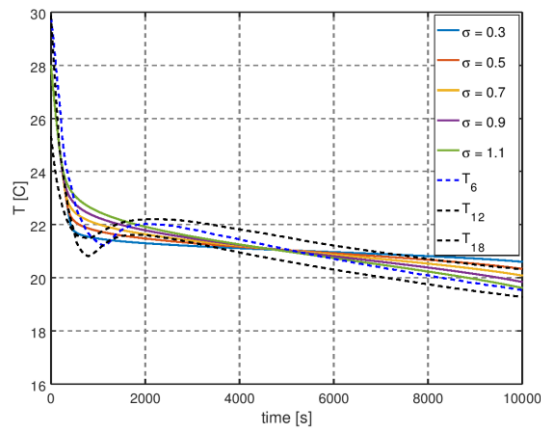


Figure 28 Solidification process temperature for $R=1.3$ W/K

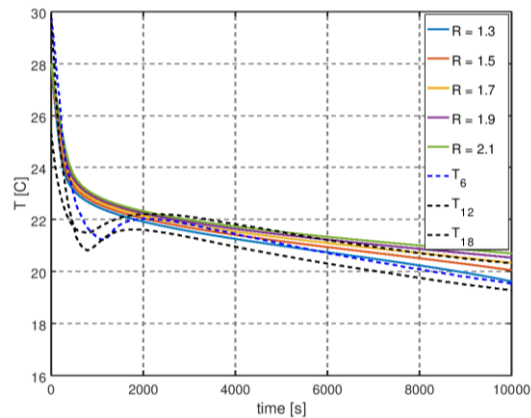


Figure 29 Solidification process temperature for $\sigma = 1.1$

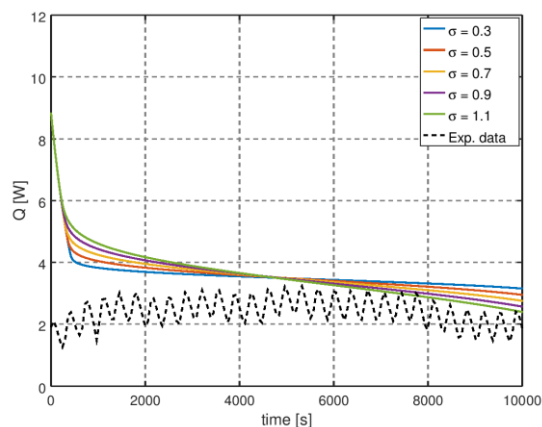


Figure 30 Solidification process time dependent heat transfer for $R=1.3$ W/K

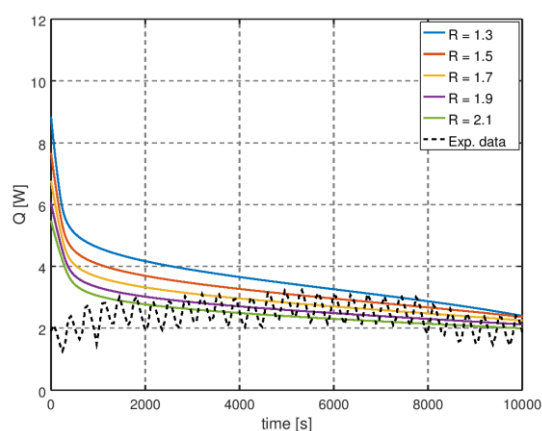


Figure 31 Solidification process time dependent heat transfer for $\sigma=1.1$

5. Conclusions

This article presents experimental investigations of coconut oil based TES module. Because the coconut oil is an organic substance mixture its properties may vary significantly, properties of coconut oil has been verified by authors. Due to the fact that especially thermally properties are crucial for properly physical model of melting solidification phenomena, that values have been determination based on a statistical sample. It has been conformed of strong influence of natural convection phenomena at the melting process. Circulation of liquid phase more effectively accelerate melting process at the top part of cylinder compare to the bottom one. The temperature field is more uniform in the areas of conduction mechanism domination. That areas has been located near outer/lower regions of tank. The melting process is more complex for mixture substance than the pure, single compound substance. It has been observed that in case of coconut oil it is better to talk about appearance melting temperature than melting temperature. What is more the range of appearance melting temperature is a function distance from heat source. However for the

same surface the melting time is the same. In case of solidification the influences of natural convection is reduce quickly due to increasing domination of conduction heat transfer mechanism. For the solidification temperature profiles are characteristic the occurrence of sub cooling temperature. The level of temperature drop in sub cooling is a function of distance from heat source. However the similar like in case of melting processes the initial time for the solidification process is the same for the same surfaces. The sinking of PCM by gravitational force influences enhances clearly solidification process in bottom part of experimental module. It should be highlight that in case of melting as well as solidification process the shape of phase-change profile seems to forms an truncated cone (in case of melting inverted).

Presented visual and own experiment has been evaluated with simple mathematical model to verify the applicability of the thermophysical data of the PCM in system behavior prediction. The goal of this analysis was to provide a simple method to predict presented module with the charging/discharging system. This simple approach is of great value during the early design stage because it allows the designer to simply evaluate the influence of the latent TES functionality on the overall system performance in an integrated manner based on minimal input parameters of the latent TES.

Based on the best fit approach the parameters thermal resistance of the module $R = 1.3\text{W/K}$ was found. Additionally the latent heat of the coconut oil of 178 kJ/kg with Gaussian distribution ($\sigma = 1.1$) for melting in temperature of 25°C and solidification in 21°C .

further works will be focused on estimation of the convection effect on the thermal resistance of the module.

Acknowledgements

This research work was supported by *National* Centre for Research and Development, Poland (Project No. LIDER/4/0008/L-9/17/NCBR/2018)

Literature

- [1] I. Dincer, On thermal energy storage systems and applications in buildings, *Energy Build.* 34 (2002) 377–388.
- [2] A. Avara, E. Daneshgar, Optimum placement of condensing units of split-type air-conditioners by numerical simulation, *Energy Build.* 40 (2008) 1268–1272.
- [3] J. Asrael, P.E. Phelan, B.D. Wood, Feasibility of lowering the condenser's inlet water temperature of a chiller using thermal water storage, *Appl. Energy.* 66 (2000) 339–356.
- [4] A. Sharma, V.V. Tyagi, C.R. Chen, D. Buddhi, Review on thermal energy storage with phase change materials and applications, *Renew. Sustain. Energy Rev.* 13 (2009) 318–345.

- [5] A. Crespo, C. Barreneche, M. Ibarra, W. Platzer, Latent thermal energy storage for solar process heat applications at medium-high temperatures – A review, *Sol. Energy*. 192 (2019) 3–34. doi:10.1016/j.solener.2018.06.101.
- [6] T.M. Letcher, R. Law, D. Reay, *Storing energy: with special reference to renewable energy sources*, Elsevier Oxford, 2016.
- [7] N.H. Jayadas, K.P. Nair, Coconut oil as base oil for industrial lubricants—evaluation and modification of thermal, oxidative and low temperature properties, *Tribol. Int.* 39 (2006) 873–878.
- [8] E. Chan, C.R. Elevitch, *Cocos nucifera (coconut)*, *Species Profiles Pacific Isl. Agrofor.* 2 (2006) 1–27.
- [9] J.C. Choi, S.D. Kim, Heat-transfer characteristics of a latent heat storage system using $MgCl_2 \cdot 6H_2O$, *Energy*. 17 (1992) 1153–1164.
- [10] A. Pizzolato, A. Sharma, K. Maute, A. Sciacovelli, V. Verda, Design of effective fins for fast PCM melting and solidification in shell-and-tube latent heat thermal energy storage through topology optimization, *Appl. Energy*. 208 (2017) 210–227.
- [11] A. Trp, K. Lenic, B. Frankovic, Analysis of the influence of operating conditions and geometric parameters on heat transfer in water-paraffin shell-and-tube latent thermal energy storage unit, *Appl. Therm. Eng.* 26 (2006) 1830–1839.
- [12] K.A.R. Ismail, M.M. Abugderah, Performance of a thermal storage system of the vertical tube type, *Energy Convers. Manag.* 41 (2000) 1165–1190.
- [13] Y.B. Tao, Y.L. He, Effects of natural convection on latent heat storage performance of salt in a horizontal concentric tube, *Appl. Energy*. 143 (2015) 38–46.
- [14] Q. Mao, N. Liu, L. Peng, Numerical Investigations on Charging/Discharging Performance of a Novel Truncated Cone Thermal Energy Storage Tank on a Concentrated Solar Power System, *Int. J. Photoenergy*. 2019 (2019).
- [15] M.J. Hosseini, A.A. Ranjbar, M. Rahimi, R. Bahrampoury, Experimental and numerical evaluation of longitudinally finned latent heat thermal storage systems, *Energy Build.* 99 (2015). doi:10.1016/j.enbuild.2015.04.045.
- [16] D. Zhao, G. Tan, Numerical analysis of a shell-and-tube latent heat storage unit with fins for air-conditioning application, *Appl. Energy*. 138 (2015) 381–392. doi:10.1016/j.apenergy.2014.10.051.
- [17] X. Yang, P. Wei, X. Wang, Y.-L. He, Gradient design of pore parameters on the melting process in a thermal energy storage unit filled with open-cell metal foam, *Appl. Energy*. 268 (2020) 115019.
- [18] X. Yang, Z. Niu, Q. Bai, H. Li, X. Cui, Y.-L. He, Experimental study on the solidification process of fluid saturated in fin-foam composites for cold storage, *Appl. Therm. Eng.* 161 (2019) 114163.
- [19] J.M. Mahdi, S. Lohrasbi, E.C. Nsofor, Hybrid heat transfer enhancement for latent-heat thermal energy storage systems: A review, *Int. J. Heat Mass Transf.* 137 (2019) 630–649.
- [20] J.M. Mahdi, S. Lohrasbi, D.D. Ganji, E.C. Nsofor, Simultaneous energy storage and recovery in the triplex-tube heat exchanger with PCM, copper fins and Al_2O_3 nanoparticles, *Energy Convers. Manag.* 180 (2019) 949–961.
- [21] Z. Hu, A. Li, R. Gao, H. Yin, Enhanced heat transfer for PCM melting in the frustum-shaped unit with multiple PCMs, *J. Therm. Anal. Calorim.* 120 (2015) 1407–1416.
- [22] H.A. Adine, H. El Qarnia, Numerical analysis of the thermal behaviour of a shell-and-tube heat storage unit using phase change materials, *Appl. Math. Model.* 33 (2009) 2132–2144.

- [23] M. De Falco, M. Capocelli, A. Giannattasio, Performance analysis of an innovative PCM-based device for cold storage in the civil air conditioning, *Energy Build.* 122 (2016) 1–10.
- [24] W.-S. Lee, Y. Chen, T.-H. Wu, Optimization for ice-storage air-conditioning system using particle swarm algorithm, *Appl. Energy.* 86 (2009) 1589–1595.
- [25] F. Agyenim, N. Hewitt, P. Eames, M. Smyth, A review of materials, heat transfer and phase change problem formulation for latent heat thermal energy storage systems (LHTESS), *Renew. Sustain. Energy Rev.* 14 (2010) 615–628.
- [26] National Instruments Corporation, *LabVIEW User Manual*, Ni.Com. (2013).
- [27] H.M. Ettouney, I. Alatiqi, M. Al-Sahali, S.A. Al-Ali, Heat transfer enhancement by metal screens and metal spheres in phase change energy storage systems, *Renew. Energy.* 29 (2004) 841–860.
- [28] S. Kahwaji, M.A. White, Edible oils as practical phase change materials for thermal energy storage, *Appl. Sci.* 9 (2019) 1627.
- [29] A. Valente, R. Morais, C. Couto, J.H. Correia, Modeling, simulation and testing of a silicon soil moisture sensor based on the dual-probe heat-pulse method, *Sensors Actuators A Phys.* 115 (2004) 434–439.
- [30] G.J. Kluitenberg, K.L. Bristow, B.S. Das, Error analysis of heat pulse method for measuring soil heat capacity, diffusivity, and conductivity, *Soil Sci. Soc. Am. J.* 59 (1995) 719–726.
- [31] B. Caballero, L.C. Trugo, P.M. Finglas, *Encyclopedia of food sciences and nutrition*, Academic, 2003.
- [32] H. Hamdani, S. Rizal, M. Riza, Numerical simulation analysis on the thermal performance of a building walls incorporating Phase Change Material (PCM) for thermal management, in: *IOP Conf. Ser. Mater. Sci. Eng.*, IOP Publishing, 2018: p. 12186.
- [33] J.C. Kurnia, A.P. Sasmito, Numerical investigation of heat transfer performance of a rotating latent heat thermal energy storage, *Appl. Energy.* 227 (2018) 542–554.
- [34] G.R. Solomon, S. Karthikeyan, R. Velraj, Sub cooling of PCM due to various effects during solidification in a vertical concentric tube thermal storage unit, *Appl. Therm. Eng.* 52 (2013) 505–511.
- [35] J.F. Belmonte, P. Eguía, A.E. Molina, J.A. Almendros-ibáñez, R. Salgado, A simplified method for modeling the thermal performance of storage tanks containing PCMs, *Appl. Therm. Eng.* 95 (2016) 394–410. doi:10.1016/j.applthermaleng.2015.10.111.
- [36] J.W. Eaton, D. Bateman, S. Hauberg, R. Wehbring, *A high-level interactive language for numerical computations Edition 4 for Octave version 4 Free Your Numbers*, (2015).